

Unprecedented Li⁺ Exchange in an Anionic Metal–Organic Framework: Significantly Enhanced Gas Uptake CapacityBo Liu,^{†,‡} Rui Zhang,[‡] Chun-Yang Pan,^{*,†} and Hai-Long Jiang^{*,‡,✉}[†]School of Light Industry and Chemical Engineering, Guangdong University of Technology, Guangzhou 510006, China[‡]Hefei National Laboratory for Physical Sciences at the Microscale, Collaborative Innovation Center of Suzhou Nano Science and Technology, Department of Chemistry, University of Science and Technology of China, Hefei, Anhui 230026, P. R. China

Supporting Information

ABSTRACT: We herein report the first example of Li⁺ exchanged with both the guest H₂N(Me)₂⁺ cations located in the channels and the coordinated metal ions from an anionic metal–organic framework (MOF), leading to significant enhancement of the pore volume and gas sorption abilities of the exchanged MOF. Furthermore, both MOFs before and after Li⁺ exchange show good selective adsorption for CO₂ over CH₄.

Metal–organic frameworks (MOFs), owing to their adjustable pore sizes and controllable pore-surface properties, present a diversity of applications in clean energy, such as hydrogen and methane storage and CO₂ capture.¹ Particularly given the increasingly serious global warming, the effective capture and removal of CO₂ from industrial flue gas is becoming an important environmental issue.² In view of the problems existing in CO₂ capture, recent studies have demonstrated that MOFs could be a promising physical adsorbent for CO₂, being an alternative to the existing benchmark materials for CO₂ capture at low concentration and moderate temperature.³ In order to enhance the CO₂ adsorption capacity and selectivity of MOFs, some strategies, such as creating high internal surface areas and large pore volumes,⁴ increasing the coordinatively unsaturated open metal sites or nitrogen-enriched Lewis basic sites,⁵ and functionalizing by postsynthetic modification,⁶ have been adopted. In this regard, the introduction of light metal ions such as Li⁰/Li⁺ into MOFs might be an effective approach to improving the gas uptake capacity. For example, lithium-doped MIL-53 was reported to exhibit nearly double the H₂ uptake capacity of pristine MOF.⁷ Eddaoudi et al.⁸ investigated the enhanced isosteric heat of H₂ adsorption in a Li⁺-exchanged Li- ρ -ZMOF. Yang et al.⁹ synthesized an interpenetrated anionic MOF by exchanging dications with Li⁺ cations to modulate the hysteretic H₂ adsorption behavior and determined the precise Li⁺ position in the Li⁺-exchange framework as important evidence for the basis of modulated H₂ uptake. In summary, chemical reduction and cation exchange are two methods to incorporate Li⁺ into MOFs that act as effective strategies to modulating H₂ adsorption in most previous studies.¹⁰

More recently, the incorporation of Li⁺ cations into MOFs for enhancing the CO₂ adsorption capacity and selectivity has aroused widespread concern.¹¹ In this contribution, we report the synthesis, structure, and exchange reactions of two MOFs,

[H₂N(Me)₂]₂[Zn₅(L)₃]·5.5DMF·3.5H₂O (**1**) and [Li(H₃O)₂]₂[Zn₄Li(L)₃]·6CH₃OH (**1-Li**), of a Zn₅(CO₂)₁₂/Zn₄Li(CO₂)₁₂ cluster-based anionic framework, together with the gas (N₂, H₂, CH₄, and CO₂) sorption properties of their desolvated forms. Notably, **1-Li** presents an unprecedented example in which the exchange interaction of Li⁺ ions take place in both the guest H₂N(Me)₂⁺ ions and the coordinated metal atoms of the host framework. In addition, the pore volume and gas uptake capability of **1-Li** show significant enhancement compared to the pristine **1**.

Compound **1** crystallizes in the monoclinic space group C2/c, showing a 3D anionic porous framework constructed from an irregular linear pentanuclear Zn²⁺ cluster and L⁴⁻ ligand. The asymmetric unit of **1** consists of two and a half Zn²⁺ ions and one and a half L⁴⁻ ions (Figure S1). All Zn²⁺ centers adopt distorted tetrahedral coordination geometries via bonding to single O centers from four carboxylate groups. L⁴⁻ adopts μ_6^- and μ_7^- , two kinds of bridging coordination modes (Figure S2). Interestingly, five linearly arranged Zn²⁺ ions are bridged by eight carboxylate groups, in which each outer Zn ion (Zn2) is further coordinated by two carboxylate O atoms from two carboxylate groups to generate a Zn₅(CO₂)₁₂ cluster (Figure 1a), presenting a new zinc carboxylate based Zn^{II} cluster. Furthermore, the Zn₅(CO₂)₁₂ cluster as a secondary building unit (SBU) incorporates eight carboxylate groups from six μ_7^- -L⁴⁻ infinitely to form 2D layers that run parallel to the *ab* plane and shows narrow 1D channels along the *c* axis that are occupied by H₂N(Me)₂⁺ cations decomposed from *N,N*-dimethylformamide (Figure 1b). The 2D layers are further linked by μ_6^- -L⁴⁻ ligands to give a 3D anionic framework (Figure 1c), and a 1D large channel B is formed with a cylindrical aperture of ca. 12.322 Å (the distance of C22...C22, including the van der Waals radii of the atoms). The void space of **1** is 55.3%, estimated by PLATON after excluding the H₂N(Me)₂⁺ cations and free solvents.¹²

To establish the influence of the cationic species on the adsorption properties, Li⁺-ion exchange was performed. To this end, crystals of as-synthesized **1** were immersed in a saturated solution of LiNO₃ in methanol at room temperature for 10 days, and the LiNO₃ solution was refreshed daily. Subsequently, the cation-exchanged crystals of **1-Li** were rinsed and soaked in methanol for 3 days to remove residual LiNO₃ from the framework. Powder X-ray diffraction (PXRD) of **1-Li** clearly revealed that the framework structure remained intact after the cation-exchange process (Figure S3). Elemental analysis of a bulk

Received: February 28, 2017

Published: April 5, 2017

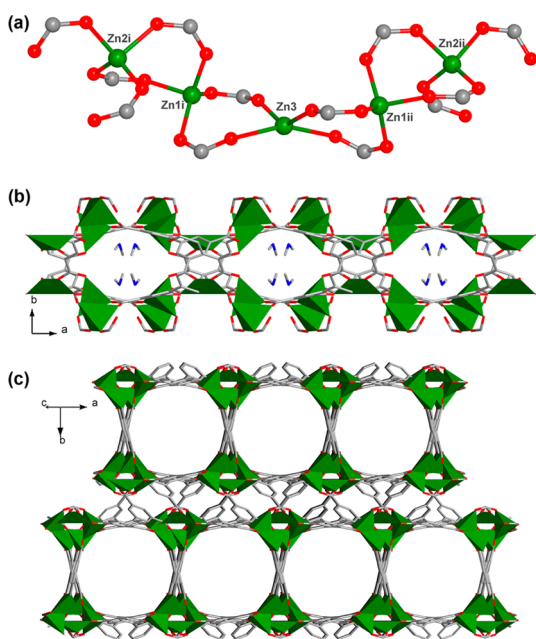


Figure 1. (a) $\text{Zn}_5(\text{CO}_2)_{12}$ cluster (symmetry codes: $i, -1 + x, y, z$; $ii, 1 - x, y, 1.5 - z$), (b) view of the 2D layer along the c axis in which the channels are filled by $\text{H}_2\text{N}(\text{Me})_2^+$ cations, and (c) view of the 3D structure.

sample of **1-Li** confirmed that no N element was detectable in the Li^+ -exchanged material, indicating that $\text{H}_2\text{N}(\text{Me})_2^+$ had been totally replaced by Li^+ and H_3O^+ within the pores of the framework. Moreover, inductively coupled plasma results demonstrated that the molar ratio between Li and Zn within **1-Li** was approximately 0.5. Especially, the single-crystal structure of **1-Li** can be obtained by single-crystal X-ray diffraction analysis (Table S1 and CIF). Significantly, in the structure of **1-Li**, not only was $\text{H}_2\text{N}(\text{Me})_2^+$ replaced by Li^+ but also the Zn^{2+} ion located in the center of the $\text{Zn}_5(\text{CO}_2)_{12}$ cluster was exchanged with Li^+ ion. This unprecedented cation-exchange process occurring to both the guest and host framework is attributed to two reasons: first, as shown in Figure 2, in the $\text{Zn}_5(\text{CO}_2)_{12}$

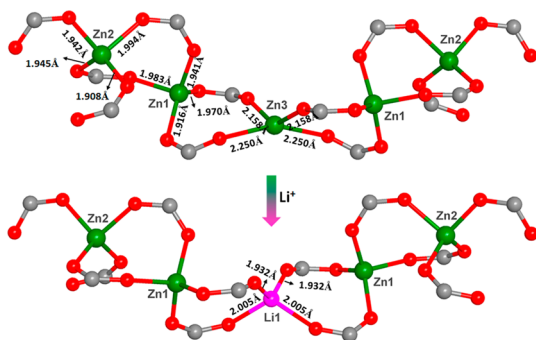


Figure 2. Bond lengths of the Zn–O and Li–O bonds in the $\text{Zn}_5(\text{CO}_2)_{12}$ and $\text{Zn}_4\text{Li}(\text{CO}_2)_{12}$ clusters.

cluster, the Zn3 atom possessing the longer Zn–O bond is more “active” than the other four Zn^{II} atoms; second, the Li^+ ion is four-coordinated in most of the Li-based MOFs¹³ and the four-coordinated Zn3 atom is exactly suitable for metal-ion exchange. Although many Li^+ -exchanged MOFs have been reported,^{7–11} only one of their structures was successfully determined by single-crystal X-ray diffraction.⁹ Herein, **1-Li** presents the first

example of Li^+ exchange with both the guest $\text{H}_2\text{N}(\text{Me})_2^+$ ions and the coordinated metal ions of the host framework, for which the structure is decided by single-crystal data.

The methanol-exchanged sample **1** and Li^+ -exchanged sample **1-Li** are stable upon heating to 150 °C under high vacuum (10^{-5} mbar) for 8 h and give fully desolvated samples, maintaining their structural integrity, as confirmed by the PXRD results (Figures S5 and S6). The N_2 sorption isotherm of **1** measured at 77 K shows an uptake of $136 \text{ cm}^3 \text{ g}^{-1}$ at 1 atm (Figure 3a),

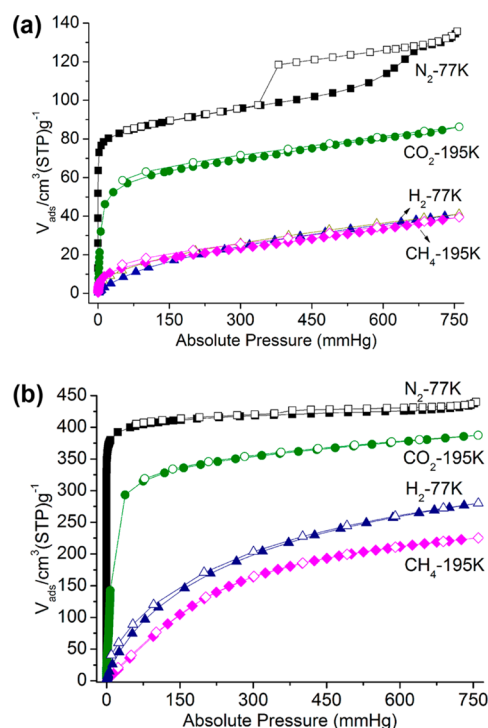


Figure 3. N_2 , H_2 , CO_2 , and CH_4 adsorption (filled) and desorption (open) isotherms of **1** (a) and **1-Li** (b) measured at 77 and 195 K.

corresponding to Brunauer–Emmett–Teller (BET) and Langmuir surface areas of 342 and $383 \text{ m}^2 \text{ g}^{-1}$, respectively. However, the isotherm of **1-Li** displays significantly higher N_2 uptake, with a maximum uptake of $440 \text{ cm}^3 \text{ g}^{-1}$ (Figure 3b). A comparison of the N_2 isotherms for **1** and **1-Li** presents a change in the isotherms from type V in **1** to type I in **1-Li**. This behavior might be due to fact that the existence of small Li^+ cations in channels of **1-Li** is not a barrier for the entrance of N_2 molecules, but the presence of large $\text{H}_2\text{N}(\text{Me})_2^+$ cations would block the channels of **1**.^{9,14} The BET and Langmuir surface areas of **1-Li** are up to 1664 and $1780 \text{ m}^2 \text{ g}^{-1}$, respectively, indicating that the adsorption capacity of **1-Li** is 3.9 times greater than that of **1**. The total pore volumes for **1** and **1-Li** calculated from the maximum N_2 adsorption are 0.21 and 0.68 g cm^{-3} , respectively. The experimental pore-size-distribution curves based on the nonlocal density functional theory model demonstrate almost the same pore-size distribution of **1** and **1-Li** (Figure S7), consistent with their similar structures. The H_2 sorption of **1-Li** exhibits a very much enhanced uptake capacity compared to that of **1**. As shown in Figure 3, the H_2 uptakes of **1** and **1-Li** at 77 K and 1 atm are $41 \text{ cm}^3 \text{ g}^{-1}$ (0.37 wt %) and $280 \text{ m}^3 \text{ g}^{-1}$ (2.50 wt %), respectively. The uptake of **1-Li** is nearly 5.8 times higher than that of **1**, indicating a high H_2 adsorption capacity of **1-Li**. It is worth noting that such a remarkable enhancement of the H_2 uptake is

Table 1. Adsorption Data for **1** and **1-Li**

	BET ^a	77 K ^b			195 K ^b		273/298 K ^b		Q _{st} (CO ₂) ^c	S(CO ₂ /CH ₄) ^d
		H ₂	CO ₂	CH ₄	CO ₂	CH ₄	CO ₂	CH ₄		
1	342	41	86	40	37/24	30/17	23.0	11		
1-Li	1664	280	388	226	148/85	35/21	20.1	9		

^aSurface area, m² g⁻¹. ^bAdsorptive capability, cm³ g⁻¹. ^cIsosteric heat of adsorption, kJ mol⁻¹. ^dSelectivity sorption at 298 K.

the largest compared with known methods utilized for modulation of the H₂ sorption.^{1c,10,15}

The above results regarding enhanced N₂ and H₂ uptake capacities of **1-Li** encourage us to examine their potential applications for CO₂ and CH₄ sorption at different temperatures (Table 1). At low temperature (195 K), the CO₂ and CH₄ uptakes of **1** are 86 and 40 cm³ g⁻¹. In sharp contrast, those values of **1-Li** reach 388 and 226 cm³ g⁻¹, respectively, at 195 K. The CO₂ and CH₄ uptakes at ambient temperature have been further investigated (Figure 4). For **1**, the CO₂ uptakes are 37 cm³ g⁻¹ at

adsorption was calculated by the virial equation from the sorption isotherms at 273 and 298 K (Figures S10 and S11). The initial Q_{st} values of CO₂ are 23.0 and 20.1 kJ mol⁻¹ for **1** and **1-Li**, respectively, suggesting that the affinity of H₂N(Me)₂⁺ cations toward CO₂ is slightly larger than that of Li⁺ cations, which is probably due to the stronger intermolecular interaction between H₂N(Me)₂⁺ and CO₂.^{10b,11d,18}

In summary, through postsynthetic ion exchange, we have achieved Li⁺ exchange with both the guest H₂N(Me)₂⁺ ions located in the pores and the coordinated metal centers of the host framework based on an anionic MOF. Furthermore, the pore volume and gas uptake capacity of the Li⁺-exchanged MOF have been greatly improved. The results presented in this study might open an avenue to improvement of the pore volume and gas uptake capacity in MOFs.

ASSOCIATED CONTENT

Supporting Information

The Supporting Information is available free of charge on the ACS Publications website at DOI: 10.1021/acs.inorgchem.7b00538.

Experimental details, additional structures, PXRD data, thermogravimetric analysis curve, and sorption data fittings (PDF)

CIF file for **1** (CIF)

CIF file for **1-Li** (CIF)

AUTHOR INFORMATION

Corresponding Authors

*E-mail: panchuny@gdut.edu.cn (C.-Y.P.).

*E-mail: jianglab@ustc.edu.cn (H.-L.J.).

ORCID

Hai-Long Jiang: 0000-0002-2975-7977

Notes

The authors declare no competing financial interest.

ACKNOWLEDGMENTS

This work was supported by the NSFC (Grants 21671044, 21371162, 21673213, and 21521001), the 973 program (Grant 2014CB931803), Star of Science and Technology of Guangdong Pearl River (Grant 201610010042), the Excellent Young Teacher Development Project of Universities in Guangdong Province (Grant YQ2015054), and China Postdoctoral Scientific Foundation (Grant 2016M602438).

REFERENCES

- (1) (a) Li, J.-R.; Kuppler, R. J.; Zhou, H.-C. Selective gas adsorption and separation in metal-organic frameworks. *Chem. Soc. Rev.* **2009**, *38*, 1477–1504. (b) Sumida, K.; Rogow, D. L.; Mason, J. A.; McDonald, T. M.; Bloch, E. D.; Herm, Z. R.; Bae, T.-H.; Long, J. R. Carbon Dioxide Capture in Metal-Organic Frameworks. *Chem. Rev.* **2012**, *112*, 724–781. (c) Suh, M. P.; Park, H. J.; Prasad, T. K.; Lim, D.-W. Hydrogen Storage in Metal-Organic Frameworks. *Chem. Rev.* **2012**, *112*, 782–

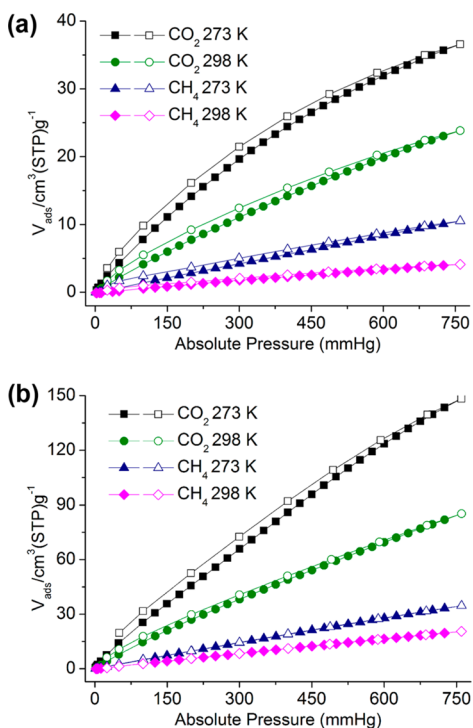


Figure 4. Sorption isotherms of CO₂ and CH₄ at 273 and 298 K for **1** (a) and **1-Li** (b). Solid and open symbols represent adsorption and desorption isotherms, respectively.

273 K and 24 cm³ g⁻¹ at 298 K at 1 atm, whereas the CH₄ uptakes are 30 and 17 cm³ g⁻¹ at 273 and 298 K, respectively. Significantly, the CO₂ isotherms of **1-Li** at 273 and 298 K reach maxima of 148 and 85 cm³ g⁻¹, respectively. In comparison, the CH₄ uptakes are 35 and 21 cm³ g⁻¹ at 1 atm, respectively, suggesting a highly selective uptake for CO₂ over CH₄. To predict the CO₂/CH₄ selectivity in **1** and **1-Li** for a CO₂/CH₄ binary mixture, the ideal adsorbed solution theory¹⁶ was employed on the basis of the adsorption curves of CO₂ and CH₄ at 298 K (Figures S8 and S9). For CO₂/CH₄ mixtures with typical feed compositions of landfill gas (CO₂/CH₄ = 50/50), the CO₂/CH₄ selectivities of **1** and **1-Li** are 11 and 9, respectively. The values are comparable to functionalized MOFs with high selectivity results.¹⁷ In addition, the isosteric heat (Q_{st}) of CO₂

835. (d) He, Y.; Zhou, W.; Qian, G.; Chen, B. Methane storage in metal–organic frameworks. *Chem. Soc. Rev.* **2014**, *43*, 5657–5678.

(2) Casper, J. K. *Greenhouse Gases: Worldwide Impacts*; Infobase Publishing: New York, 2010.

(3) Belmabkhout, Y.; Guillemin, V.; Eddaoudi, M. Low concentration CO₂ capture using physical adsorbents: Are metal–organic frameworks becoming the new benchmark materials? *Chem. Eng. J.* **2016**, *296*, 386–397.

(4) (a) Zhao, X.; Bu, X.; Zhai, Q.-G.; Tran, H.; Feng, P. Pore Space Partition by Symmetry-Matching Regulated Ligand Insertion and Dramatic Tuning on Carbon Dioxide Uptake. *J. Am. Chem. Soc.* **2015**, *137*, 1396–1399. (b) Wang, X.-S.; Chrzanowski, M.; Kim, C.; Gao, W.-Y.; Wojtas, L.; Chen, Y.-S.; Zhang, X. P.; Ma, S. Quest for highly porous metal–metalloporphyrin framework based upon a custom-designed octatopic porphyrin ligand. *Chem. Commun.* **2012**, *48*, 7173–7175.

(5) (a) Nugent, P. S.; Rhodus, V. L.; Pham, T.; Forrest, K.; Wojtas, L.; Space, B.; Zaworotko, M. J. A Robust Molecular Porous Material with High CO₂ Uptake and Selectivity. *J. Am. Chem. Soc.* **2013**, *135*, 10950–10953. (b) Liu, B.; Yao, S.; Shi, C.; Li, G.; Huo, Q.; Liu, Y. Significant enhancement of gas uptake capacity and selectivity via the judicious increase of open metal sites and Lewis basic sites within two polyhedron-based metal–organic frameworks. *Chem. Commun.* **2016**, *52*, 3223–3226. (c) Liu, B.; Zhou, H.-F.; Hou, L.; Zhu, Z.; Wang, Y.-Y. A chiral metal–organic framework with polar channels: unique interweaving six-fold helices and high CO₂/CH₄ separation. *Inorg. Chem. Front.* **2016**, *3*, 1326–1331. (d) Jiang, Z.-R.; Wang, H.; Hu, Y.; Lu, J.; Jiang, H.-L. Polar Group and Defect Engineering in a Metal–Organic Framework: Synergistic Promotion of Carbon Dioxide Sorption and Conversion. *ChemSusChem* **2015**, *8*, 878–885. (e) Li, P.-Z.; Wang, X.-J.; Zhang, K.; Nalaparaju, A.; Zou, R.; Zou, R.; Jiang, J.; Zhao, Y. Click[®]-extended nitrogen-rich metal–organic frameworks and their high performance in CO₂-selective capture. *Chem. Commun.* **2014**, *50*, 4683–4685.

(6) (a) Bloch, W. M.; Babarao, R.; Hill, M. R.; Doonan, C. J.; Sumbly, C. J. Post-synthetic Structural Processing in a Metal–Organic Framework Material as a Mechanism for Exceptional CO₂/N₂ Selectivity. *J. Am. Chem. Soc.* **2013**, *135*, 10441–10448. (b) Hu, Y.; Verdegaal, W. M.; Yu, S.-H.; Jiang, H.-L. Alkylamine-Tethered Stable Metal–Organic Framework for CO₂ Capture from Flue Gas. *ChemSusChem* **2014**, *7*, 734–737.

(7) Mulfort, K. L.; Hupp, J. T. Chemical Reduction of Metal–Organic Framework Materials as a Method to Enhance Gas Uptake and Binding. *J. Am. Chem. Soc.* **2007**, *129*, 9604–9605.

(8) Nouar, F.; Eckert, J.; Eubank, J. F.; Forster, P.; Eddaoudi, M. Zeolite-like Metal–Organic Frameworks (ZMOFs) as Hydrogen Storage Platform: Lithium and Magnesium Ion-Exchange and H₂-(rho-ZMOF) Interaction Studies. *J. Am. Chem. Soc.* **2009**, *131*, 2864–2870.

(9) Yang, S.; Lin, X.; Blake, A. J.; Walker, G. S.; Hubberstey, P.; Champness, N. R.; Schröder, M. Cation-induced kinetic trapping and enhanced hydrogen adsorption in a modulated anionic metal–organic framework. *Nat. Chem.* **2009**, *1*, 487–493.

(10) (a) Yang, S.; Lin, X.; Blake, A. J.; Thomas, K. M.; Hubberstey, P.; Champness, N. R.; Schröder, M. Enhancement of H₂ adsorption in Li⁺-exchanged co-ordination framework materials. *Chem. Commun.* **2008**, 6108–6110. (b) Gong, Y.-N.; Meng, M.; Zhong, D.-C.; Huang, Y.-L.; Jiang, L.; Lu, T.-B. Counter-cation modulation of hydrogen and methane storage in a sodalite-type porous metal–organic framework. *Chem. Commun.* **2012**, *48*, 12002–12004. (c) Qian, J.; Jiang, F.; Yuan, D.; Li, X.; Zhang, L.; Su, K.; Hong, M. Increase in pore size and gas uptake capacity in indium-organic framework materials. *J. Mater. Chem. A* **2013**, *1*, 9075–9082.

(11) (a) Liu, Y.; Wang, Z. U.; Zhou, H.-C. Recent advances in carbon dioxide capture with metal-organic frameworks. *Greenhouse Gases: Sci. Technol.* **2012**, *2*, 239–259. (b) Bae, Y.-S.; Hauser, B. G.; Farha, O. K.; Hupp, J. T.; Snurr, R. Q. Enhancement of CO₂/CH₄ selectivity in metal-organic frameworks containing lithium cations. *Microporous Mesoporous Mater.* **2011**, *141*, 231–235. (c) Babarao, R.; Jiang, J. W. Cation Characterization and CO₂ Capture in Li⁺-Exchanged Metal–Organic Frameworks: From First-Principles Modeling to Molecular Simulation. *Ind. Eng. Chem. Res.* **2011**, *50*, 62–68. (d) Huang, Y.-L.; Jiang, L.; Lu, T.-

B. Modulation of Gas Sorption Properties through Cation Exchange within an Anionic Metal–Organic Framework. *ChemPlusChem* **2016**, *81*, 780–785. (e) Bai, L.; Tu, B.; Qi, Y.; Gao, Q.; Liu, D.; Liu, Z.; Zhao, L.; Li, Q.; Zhao, Y. Enhanced performance in gas adsorption and Li ion batteries by docking Li⁺ in a crown ether-based metal–organic framework. *Chem. Commun.* **2016**, *52*, 3003–3006.

(12) Spek, A. L. J. Single-crystal structure validation with the program PLATON. *J. Appl. Crystallogr.* **2003**, *36*, 7–13.

(13) Clough, A.; Zheng, S.-T.; Zhao, X.; Lin, Q.; Feng, P.; Bu, X. New Lithium Ion Clusters for Construction of Porous MOFs. *Cryst. Growth Des.* **2014**, *14*, 897–900.

(14) Li, Z.-J.; Khani, S. K.; Akhbari, K.; Morsali, A.; Retailleau, P. Achieve to easier opening of channels in anionic nanoporous metal–organic framework by cation exchange process. *Microporous Mesoporous Mater.* **2014**, *199*, 93–98.

(15) (a) Murray, L. J.; Dincă, M.; Long, J. R. Hydrogen storage in metal–organic frameworks. *Chem. Soc. Rev.* **2009**, *38*, 1294–1314. (b) Sculley, J.; Yuan, D.; Zhou, H.-C. The current status of hydrogen storage in metal–organic frameworks—updated. *Energy Environ. Sci.* **2011**, *4*, 2721–2735.

(16) Myers, A. L.; Prausnitz, J. M. Thermodynamics of mixed-gas adsorption. *AIChE J.* **1965**, *11*, 121.

(17) (a) Liu, Y.; Li, J.-R.; Verdegaal, W. M.; Liu, T.-F.; Zhou, H.-C. Isostructural Metal–Organic Frameworks Assembled from Functionalized Diisophthalate Ligands through a Ligand-Truncation Strategy. *Chem. - Eur. J.* **2013**, *19*, 5637–5643. (b) Hu, Z.; Nalaparaju, A.; Peng, Y.; Jiang, J.; Zhao, D. Modulated Hydrothermal Synthesis of UiO-66(Hf)-Type Metal–Organic Frameworks for Optimal Carbon Dioxide Separation. *Inorg. Chem.* **2016**, *55*, 1134–1141. (c) Wang, B.; Huang, H.; Lv, X.-L.; Xie, Y.; Li, M.; Li, J.-R. Tuning CO₂ Selective Adsorption over N₂ and CH₄ in UiO-67 Analogues through Ligand Functionalization. *Inorg. Chem.* **2014**, *53*, 9254–9259.

(18) (a) Choi, M. H.; Park, H. J.; Hong, D. H.; Suh, M. P. Comparison of Gas Sorption Properties of Neutral and Anionic Metal–Organic Frameworks Prepared from the Same Building Blocks but in Different Solvent Systems. *Chem. - Eur. J.* **2013**, *19*, 17432–17438. (b) Liao, P.-Q.; Chen, X.-W.; Liu, S.-Y.; Li, X.-Y.; Xu, Y.-T.; Tang, M.; Rui, Z.; Ji, H.; Zhang, J.-P.; Chen, X.-M. Putting an ultrahigh concentration of amine groups into a metal–organic framework for CO₂ capture at low pressures. *Chem. Sci.* **2016**, *7*, 6528–6533.